

## The molecular docking study on interaction several suggested potential drug candidates on COVID-19 disease

Daryoush Afzali <sup>\*1</sup>, Behnoosh Bahadori <sup>1</sup>, Zahra Afzali<sup>2</sup>

<sup>1</sup> Department of Environment, Institute of Science and High Technology and Environmental Sciences, Graduate University of Advanced Technology, Kerman, Iran

<sup>2</sup> Department of Nanotechnology, Graduate University of Advanced Technology, Kerman, Iran

**Corresponding author:** daryoush\_afzali@yahoo.com, d.afzali@kgut.ac.ir

**Received:** 10 July 2024

**Accepted:** 22 August 2024

**DOI:** [10.30473/ijac.2026.77143.1338](https://doi.org/10.30473/ijac.2026.77143.1338)

### Abstract

A novel coronavirus (CoV), SARS-CoV-2 surfaced in late 2019 in Wuhan, China and spread across whole world. We started a study on COVID-19 and several clinical inhibitors, firstly we did molecular simulation on COVID-19 by Gromacs tools. Then simulated conformation was docked with suggested drugs for confirmation docking. The molecular docking results were similar to X-ray crystallography results in protein data bank and the analyses were confirmed by this method. The resulting conformation of the reported drugs with the COVID-19 was used for docking analyses. Furthermore, to study receptor conformation stability, a second MD simulation on complex was performed in an aqueous environment. RMSD for complex showed that the COVID19 conformation did not change in the presence of the suggested drugs. The results of docking showed that estimated free energy of binding, final intermolecular energy and hydrogen bond play an important role in interaction between suggested drugs and COVID-19. The results emerging docking showed that Sofosbuvir, vitamin D and 2aurintricarboxylic acid have been potential to be applied as new COVID-19 anti corona virus drugs.

**Keywords:** Docking Analyses, Molecular Dynamic, Simulation

### 1. INTRODUCTION

The world is watching an unprecedented scientific race to find effective treatments against the disease caused by the new coronavirus (Sars nCov2) which is an etiological agent responsible for the viral pneumonia outbreak from early December 2019 to the present day [1]. This outbreak began with several unexplained cases of pneumonia reported in Wuhan city, Hubei province in China, in December 2019 [2]. Currently, there are no therapeutic measures aimed at combating it, and effective treatment options are still limited. Notably, Sars nCov2 provides a new strain for a disease or half of its genome [3-5], without close genetic relationships with other viruses within the sarbecovirus subgenus [6, 7]. This genomic part also comprises half of the peak region that encodes a multifunctional protein [8, 9] also responsible for the entry of the virus into host cells [10, 11]. The unique genetic characteristics of COVID-19 and its potential association with virus characteristics and

virulence in humans have yet to be elucidated [12, 13]. The Coronaviridae family includes a large number of viruses that are found in nature in fish, birds, and mammals [14]. Human coronaviruses, first characterized in the 1960s, are associated with a large percentage of respiratory infections in children and adults' [15]. Scientific interest in coronaviruses increased exponentially after the emergence of SARS Coronavirus (SARS-CoV) in southern China [16]. A similar virus was later found in horseshoe bats [17]. After the SARS epidemic, bats were considered a potential species of the reservoir that could be involved in future coronavirus-related human pandemics [17]. Thus, analyzing laboratory-confirmed cases were reported in the Middle East, during 2012, the Middle East respiratory coronavirus (MERS-CoV) appeared in Saudi Arabia [18], since then, it has killed 919 of the 2521 (35%) affected people [19]. Since SARS and MERS-CoV due to high mortality rates are prioritized along with highly pathogenic

\* Corresponding author: daryoush\_afzali@yahoo.com, d.afzali@kgut.ac.ir, Tel: +9834337776611

coronaviral diseases other than MERS and SARS [20, 21] under the Research and Development Project published by WHO. In general, coronaviruses (CoVs) are classified into four main genera [22, 23]: Alphacoronavirus, Beta coronavirus (which mainly infect mammals), Gamma coronavirus and Delta coronavirus (which mainly infect birds). By the end of 2019, six types of human nCoV were identified [24] HCoV-NL63, HCoV-229E [25], belonging to the general Alphacoronavirus, HCoV-OC43, HCoV-HKU1, SARS-CoV severe acute respiratory syndrome, and Middle Eastern respiratory syndrome MERS-CoV, belonging to the five genera of Beta coronavirus [26]. Of the CoVs mentioned, the last two are the most dangerous and were associated with the outbreak of two epidemics in the early 21st century. On January 7, 2020, COVID-19 was isolated and announced as a new seventh type of human coronavirus. In this work, we will do molecular docking (DOC), simulating the interaction of these ligands, in this case, remdesivir, umifenovir, brincidofovir, sofosbuvir, tenofovir, vitamin D, molnupiravir, fleximer and ribavirin to inhibit COVID-19.

## 2. Methodology

First of all, molecular dynamics simulation was performed by gromacs tools [27]. Docking studies were done by auto dock and BINding ANAlyzer (BINANA) tools ([28, 29]. Visual inspections were carried out by LIGPLOT (EMBL-EBI, Hinxton, Cambridgeshire, CB10 1SD) binding mode analyses were performed using the scripts within LIGPLOT tool. MVD (was used to produce 3-D figures [30, 31].

### 2.1. Preparation of data set

The structures of these drugs are shown in Fig. 1 and Table 1. The chemical structure of the drugs was constructed in Hyperchem and after that all of them optimized by PRODRG [32]. Energy minimization of these drugs was done using the AM1 semi-empirical method with the Polak-Ribiere algorithm until a root-mean-square gradient of 0.01 kcal mol<sup>-1</sup> was achieved. The resulted geometries were used for the docking study and modified by PRODRG [33].

The X-ray crystal structure for COVID-19 was selected pdb bank server were introduced. It is in complex with Z456117795 at 2.7 °A resolution was identified by Fearon and stored in the protein data bank (PDB ID code: 5R7Y).

### 2.2. Molecular dynamics simulation

Molecular dynamics simulation was performed; the structure of COVID-19 was simulated in a water box. The MD simulation process was carried out by the GROMACS 4.5.1 package using the GROMOS-96 force field.<sup>23</sup> Water molecules were added using a simple point charge (SPC216) model [34]. Counter-ions were added by replacing solvent molecules in order to neutralize the system. The system was then placed in a cubic box with the dimensions 8.63×8.63×8.63 nm<sup>3</sup> containing 63413 atoms in total. Periodic boundary conditions were applied in the xyz space. Initially, energy minimization was performed before implementing the position restraint procedure. Then, NVT and NPT simulations were carried out. The NVT simulation was performed at a constant 310 K with a Nose-Hoover thermostat. Once the temperature was stabilized, the NPT simulation was performed using the Parrinello- Rahman pressure coupling under a pressure of 1 bar. The particle mesh Ewald (PME) method interaction was used. For numerical integrations, the velocity verlet algorithm was used<sup>26</sup> and the initial atomic velocities were generated using a Maxwellian distribution at the given absolute temperature. Finally, the full system was subjected to 6000 ps MD at 310 K under 1 bar pressure. The MD simulation and result analyses were performed on the open SUSE 11.3 Linux on an Intel Core 2 Quad Q6600 2.4 GHz with 4 GB of RAM.

In the next step, simulations were performed in a constant number of molecules, pressure, and temperature by using the Berendsen thermostat at the temperature 300 K and pressure 1 bar, respectively. MD simulation studies consist of equilibration and production phases. In the first stage of equilibration, the solute (protein and counter ion) was fixed and the position-restrained dynamics simulation of the system was done at 300 K. The water and the counter ion were permitted to relax about the protein. The relaxation time of water was 20 ps. Finally, the full system was subjected to 6000 ps MD at 300 K temperature and 1 bar pressure. The periodic boundary condition was used, and the motion equations were integrated by applying the leap-frog algorithm with a time step of 2 fs. The atom coordinates were recorded every 1 ps during the simulation for latter analysis. The MD simulation lasted 5 ns to ensure that the whole systems were stable.

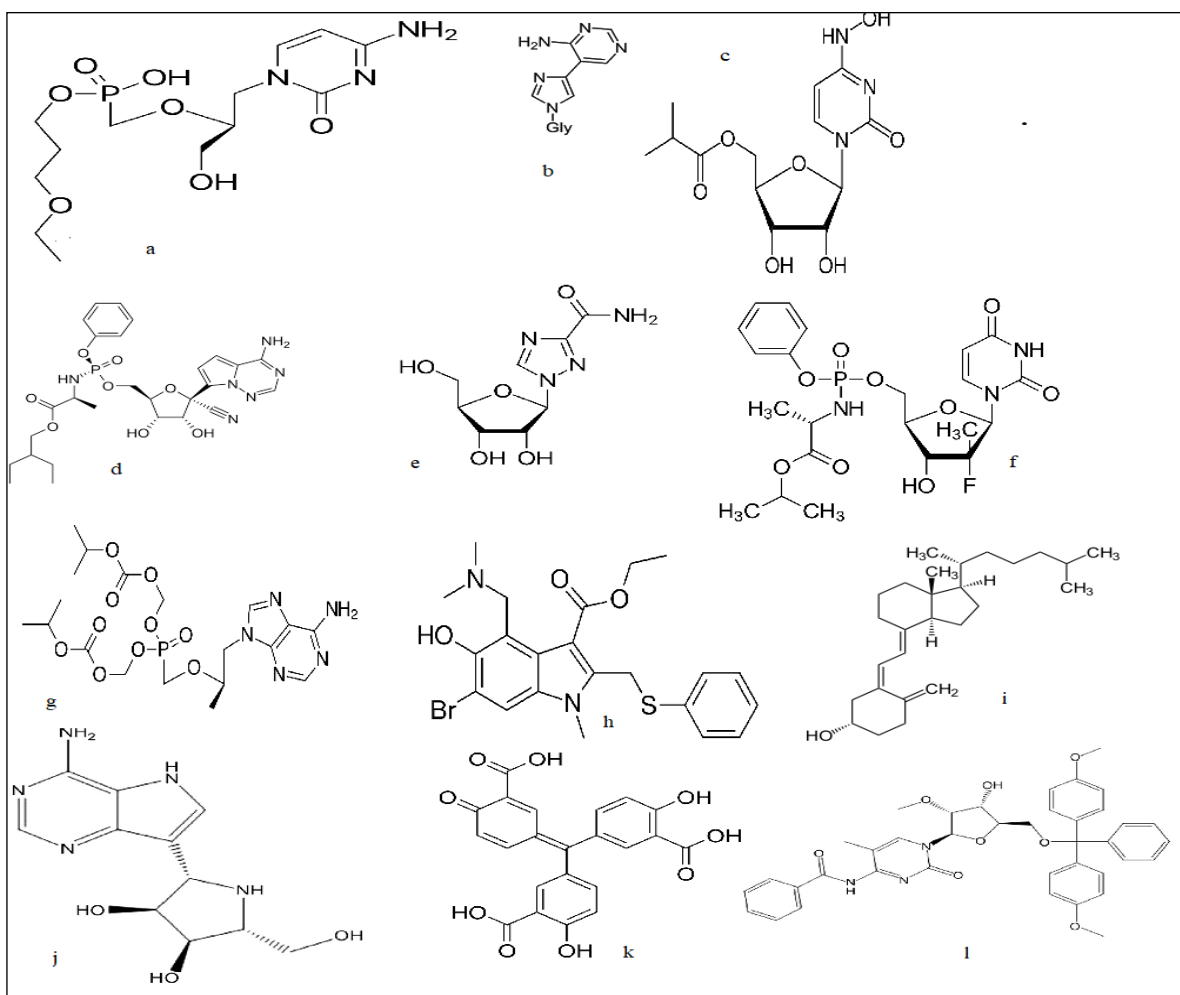


Fig. 1. The structures of reported drugs.

Table 1. Reported drugs

<b>a</b>	Brincidofovir
<b>b</b>	Feleximer
<b>c</b>	MOLNUPIRAVIR
<b>d</b>	Remdisiver
<b>e</b>	Ribavirin.svg
<b>f</b>	Sofosbuvir
<b>g</b>	Tenvirovir
<b>h</b>	Umifenovir
<b>i</b>	Vitamin D
<b>j</b>	BCX4430 (Immucillin-A)
<b>k</b>	Aurintricarboxylic ACID (ATA)
<b>l</b>	N4-Benzoyl-5'-O-(dimethoxytrityl)-5-methyl-2'-O-methylcytidine (Bz-DMT-dc)

### 2.3. Binding site refinement

To validate the reliability of the docking methodology adopted herein, the Z456117795 molecules in the X-ray crystallographic structure of 5R7Y pdb were taken as a testing molecule. Z456117795 were removed from the binding site and redocked to COVID-19 a by the blind docking, and the docked pose was compared with the crystal structure pose by calculating the RMSD value. The molecular docking results revealed that the binding site of Z456117795, obtained by auto dock tools, was similar to that of the crystal complex with an RMSD of 0.37 and 1.45 Å, respectively (Fig. 2). The results indicate that the docking method with the auto dock tools is valid.

The applied box size for docking was 82×86×126 angstroms and grid resolution were 0.375 °A. The residues of the binding site were obtained His 41, Cys 44, ser46, Met 49, His 164, Met 165, Arg188, Gln 189.

The hydrogen bond interactions are produced by the close contacts between electronegative atom (nitrogen, oxygen and ...) and hydrogen atom (hydrogen bond distance is 3.05 °A) and the hydrophobic interactions are generated by the close contacts between the non-polar amino acid side chains of the enzyme and the lipophilic groups of the inhibitor. These results clearly indicate that that Estimated free energy of binding, final intermolecular energy and hydrogen bond can affect the drugs activity of COVID-19 inhibitors, and it is suggested that more H-bond and hydrophobic interactions with the binding site could improve the drugs activity of the drugs [34].

### 2.4. Docking studies

Molecular docking was performed by auto dock 4.0 program using the Lamarckian Genetic Algorithm (LGA) method [35]. Docking parameters for the LGA were selected as population size of 150 individuals, 2.5 million energy evaluations, maximum of 27,000 generations, number of top individuals to survive to next generation of 1, mutation rate of 0.02, crossover rate of 0.8, 25 docking runs, and random

initial positions and conformations. The probability of performing a local search for an individual to the population was set to 0.06 [36]. Auto dock is a suitable program for actual docking simulation [37]. To more confidence all drugs were docked by auto dock vina too. A grid map of the size applied was the same as auto dock tools with a grid-point spacing of 1Å.

Then a set of 12 reported drugs was docked into COVID-19 model. The grid box settings were the same as those used for Z456117795.

All drugs were subsequently docked into the binding site obtained from the COVID-19 and conformation of the reported drugs with the lowest binding free energy with most populations and lowest affinity for auto dock tools and Vina tools subsequently were chosen for analyzing.

### 2.5. Descriptor calculation

Descriptors were calculated based on drugs–COVID19 interactions (structure-based) using auto dock and auto dock vina.

Auto dock computed eight types of energy values that consisted of: (1) estimated free energy of binding (EFreeBind), (2) van der Waals (vdW) + hydrogen bonding (Hbond) + desolvation energy (desolv), (3) final intermolecular energy (EInterMol) including vdW, Hbond, desolvation, and electrostatic energies, (4) electrostatic energy (EElec), (5) final total internal energy (EFTot), (6) torsional free energy (ETors), (7) Estimated Inhibition Constant, Ki and (8) the unbound system's energy (EUnb) and the Gasteiger charge descriptor. Auto dock vina computed Affinity.

Then, the docking conformer at its lowest binding energy was loaded into Molgero virtual docker to calculate the descriptors. Molgero descriptors consist of (i) close contacts; Molgero determined all ligand and protein residue that come within 2.5 and 4 °A of each other; (ii) electrostatic interactions; (iii) hydrogen bonds; (iv)hydrophobic contacts. The major descriptors were calculated from the interactions of suggested drugs with the COVID-19 showed in Table 2.

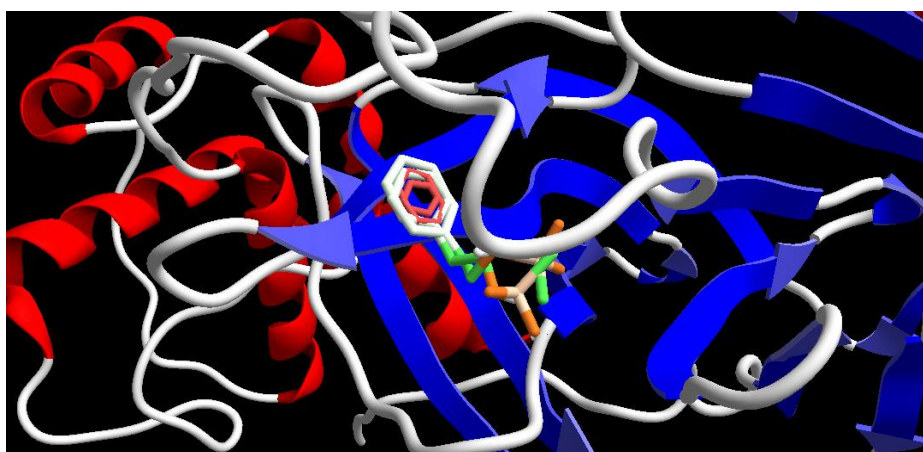


Fig. 2. Binding site refinement

Table 2. The major descriptors were calculated from the interactions of suggested drugs with the COVID-19.

symbol	Affinity (kcal/mol)	Estimated Inhibition Constant, Ki (micromolar)	H- bond	Estimated Free Energy of Binding (kcal/mol)	Final Intermolecul ar Energy (kcal/mol)	Final Total Internal Energy (kcal/mol)	Electrostat ic Energy (kcal/mol)	Torsional Free Energy (kcal/mol)
<i>f</i>	-8.2	67.64	5	-8.65	-9.54	-0.87	-0.99	+2.39
<i>k</i>	-8.0	55.23	5	-8.40	-9.89	+0.65	+0.91	+1.49
<i>i</i>	-8.0	58.29	5	-7.93	-9.43	-0.76	+0.98	+1.19
<i>l</i>	-7.8	48.57	3	-5.88	-8.46	-0.64	-0.76	+3.58
<i>c</i>	-7.8	68.59	4	-5.68	-8.98	-0.05	-0.96	+0.30
<i>g</i>	-7.5	91.02	3	-5.34	-7.92	-0.18	-0.48	+1.79
<i>d</i>	-7.1	142.11	3	-5.25	-7.42	-1.02	-0.02	+4.18
<i>b</i>	-7.1	98.09	2	-5.43	-6.92	-0.59	-0.10	+0.89
<i>e</i>	-6.8	102.02	3	-5.05	-6.04	-0.05	00.00	+0.60
<i>h</i>	-6.8	101.72	2	-5.05	-6.83	-1.42	-0.00	+2.39
<i>j</i>	-6.8	140.97	1	-5.99	-6.58	-0.42	-0.04	+0.60
<i>a</i>	-5.8	101.53	1	-3.54	-7.12	-0.22	-0.09	3.58

### 3. Results and discussion

#### 3.1. Molecular Dynamic

To provide conformation of COVID-19 in a water environment, a 6000 ps MD simulation was carried out on COVID-19 in a water box. The stability of the system (protein, water, and ions) was tested by means of the root mean square deviations (RMSD's) of protein with respect to protein's initial structure. The RMSD values of COVID-19 were plotted from 0 to 6000 ps which imply that the RMSD of the system reaches equilibrium and oscillates around 0.302 nm after 3000 ps of the simulation onset. (Fig. 3) The average RMSD value of protein backbone was calculated to be  $0.302 \pm 0.015$  nm. The RMSD value indicates that COVID-19 conformation reached equilibrium after 3800 ps in a water environment. The equilibrated conformation of the receptor was used for docking. 54

#### 3.2. Docking studies

Docking was performed by auto docks program using the Lamarckian genetic algorithm (LGA) method. As be mentioned auto dock is a suitable program for actual docking simulation. The docking studies were done for the obtained reported drugs for COVID-19.

Then, the docking poses were ranked based on their docking scores and it was selected as the best conformer of drugs by using score. The most potent drugs were chosen based on docking descriptors. Two and three-dimensional images of the binding site were produced using the LIGPLOT tools and also produced using the Molgro virtual docker (MVD) package (Molegro ApS, Denmark) respectively. The docking of the most potent drugs with the COVID-19 is shown in Fig. 4.

#### 3.3. Analysis of docking

Analysis of the suggested drugs binding locations for the COVID-19 revealed that, whereas the reported drugs docked to the orthosteric site of COVID-19. As already mentioned, 9 descriptors were calculated for the reported drugs based on drug-Covid19 interactions using auto dock tools. These most important descriptors were estimated free energy of binding, final intermolecular energy, hydrogen bond and electrostatic energies (A summed electrostatic energy is calculated using the Gasteiger partial charges by auto dock Tools). The results of docking studies on 12 reported drugs show in the table 2. The most potent drugs were Sofosbuvir, vitamin D and 2aurintricarboxylic. It showed the smaller the  $K_i$ , the greater the binding

affinity and the smaller amount of medication needed in order to inhibit the activity of that enzyme. (Table 2).

Some results showed in the Fig. 4 and 5.

#### 3.4. Molecular dynamics simulation of the COVID19-drug complex

The MD simulation on the most potent drug–COVID19 complex was done to study the effects of drugs on the COVID-19 conformation. The topology factors of sofosbuvir were built using the Dundee PRODRG2.5 server. PRODRG server select bonded parameters and atom types correctly. The complex from docking was selected as a representative for 6000 ps MD simulation in a water box as shown in Fig. 3. Analysis of the Fig. 3 indicated that the RMSD of the system reaches equilibration around an average value after 3000 ps simulation time. The stability of COVID-19 conformation was confirmed by the analysis of RMSD values (Fig. 3). The average value of RMSD for the complex was  $0.350 \pm 0.026$  nm. Therefore, it was concluded that the conformation of the COVID-19 in the presence of sofosbuvir has stabled. This stability confirmed the docking results.

### 5. Conclusion

COVID-19 that can correctly identify active compounds are important tools for rational drug design. In this study, docking molecular combined with molecular dynamic were developed to predict activity of reported drugs for COVID-19. We have simulated human COVID-19 model based upon a crystal structure and gromacs tools to stable COVID-19 in a water environment. Then molecular docking was carried out to explore the binding site. After docking of the most potent drugs of COVID-19 Sofosbuvir, the residues of the binding site obtained were His 41, Met 49, Asn 142, Gly 143, Cys 145, His 164, Met165, Glu166, Pro 168, Asp 187, Arg188, Gln 189, Thr 190, Glu192 in the cavity of the COVID-19. The selected descriptors and docking analyses indicated that active-site flexibility, hydrophobicity, summed electrostatic energy, numbers of atom-type pair counts at a distance of 4.0  $\text{\AA}$  and torisonal free energy play important roles in the COVID-19-drugs complex.

We hope it be served as a useful guideline for further treatment and designing of new compounds as COVID-19 inhibitors.

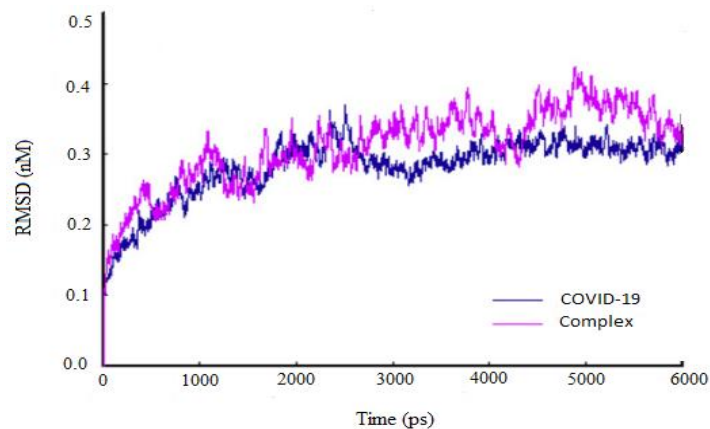
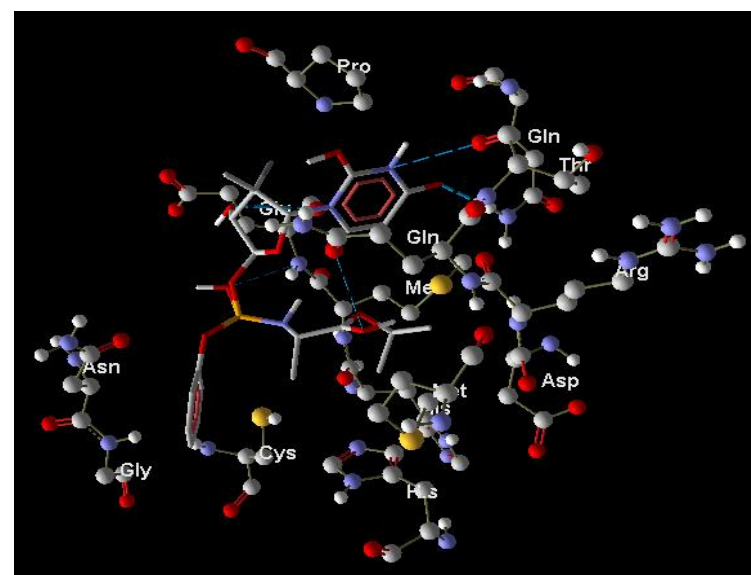
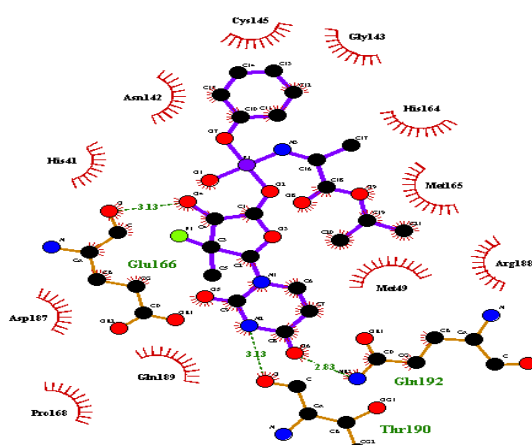


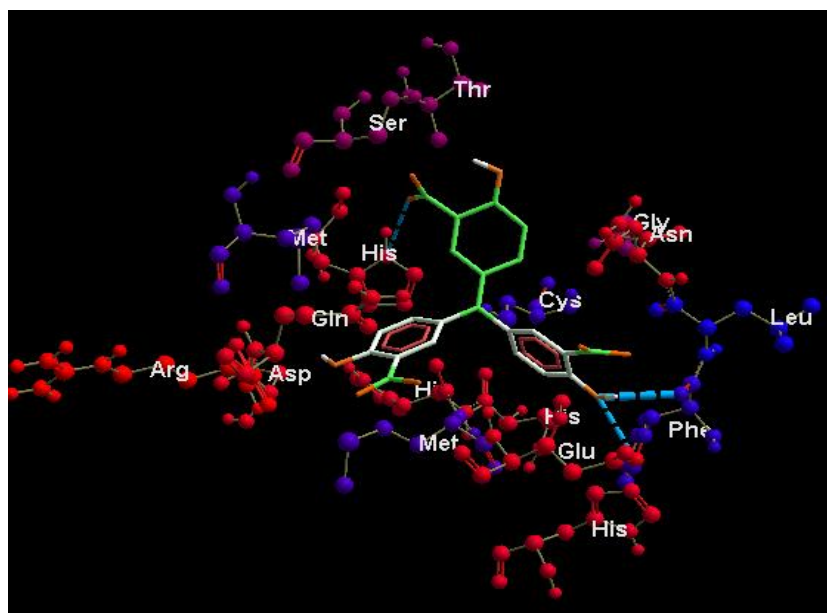
Fig. 3. RMSD values of protein backbone for COVID-19 and COVID-19 complex during 6000 ps MD simulation.



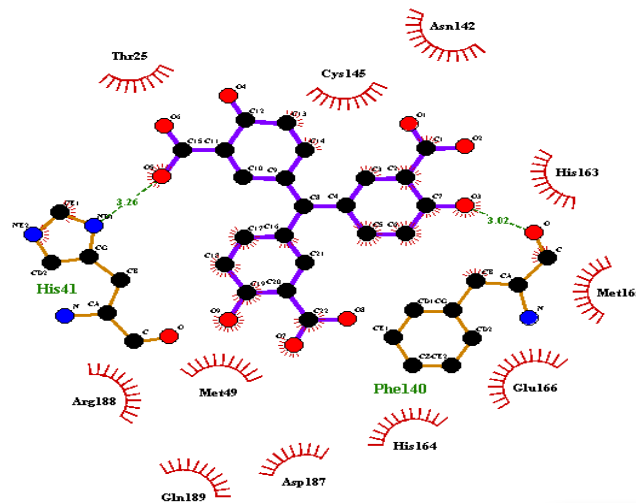
Compound f: Using MVD



Compound f: Using ligPlot

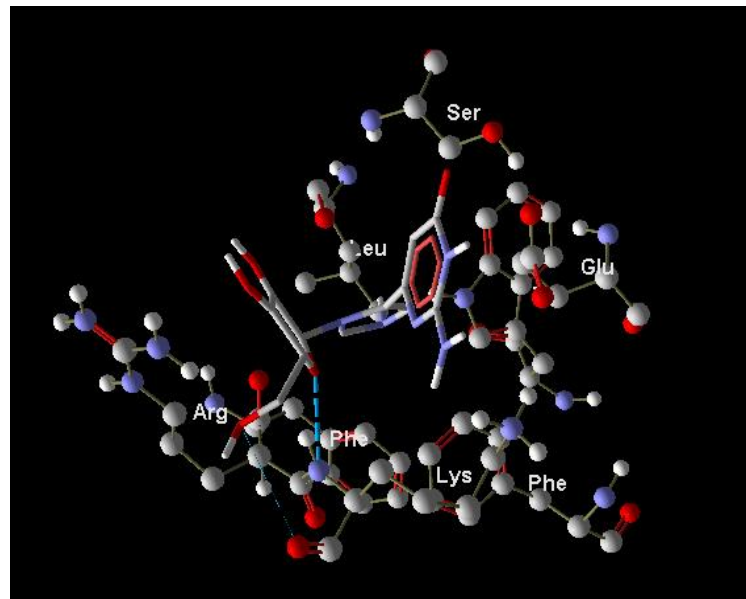


Compound k: using MVD

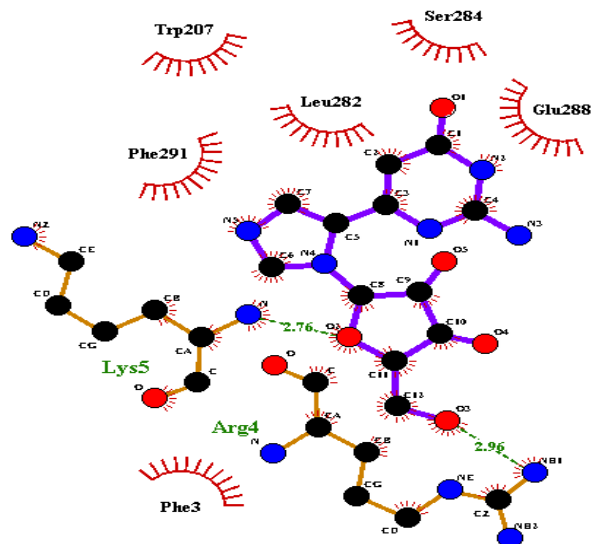


Compound k: using ligPlot

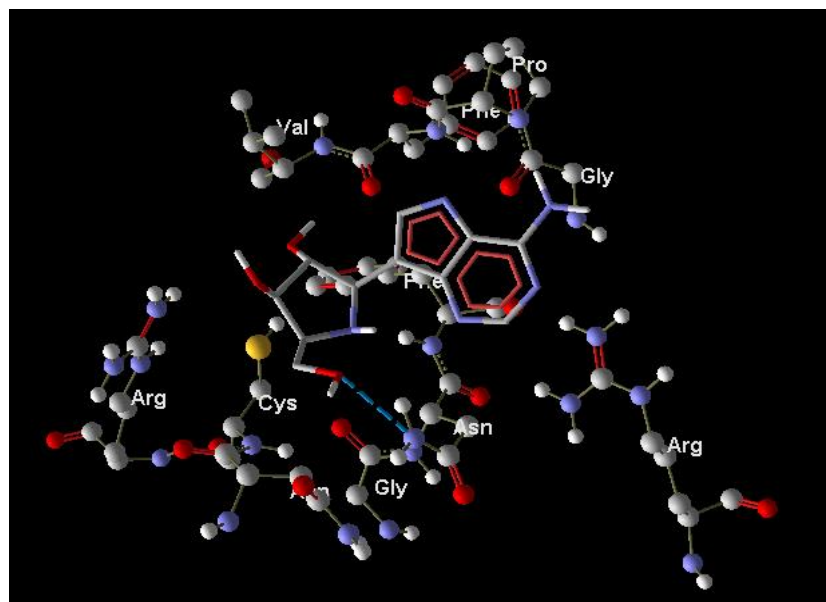
Fig. 4. The docking of the most potent inhibitors (compound f, k), 1: using MVD, 2: using ligplot



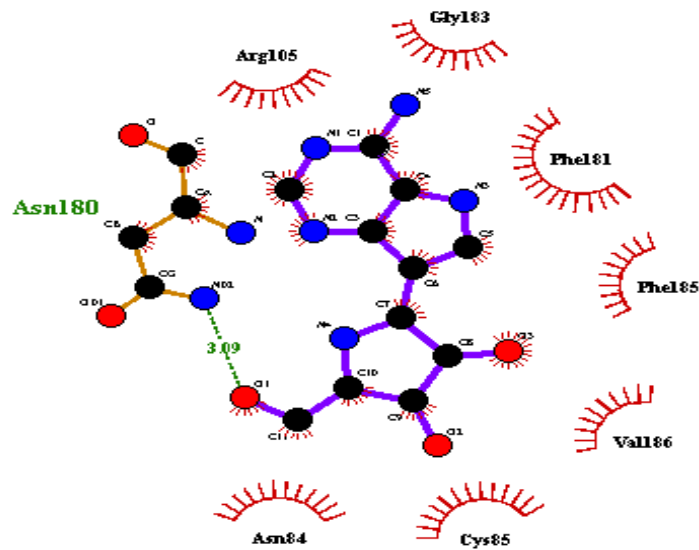
compound a: using MVD



compound a: using ligplot



compound j: using MVD



compound j: using ligplot

Fig. 5. The docking of the least potent inhibitors (compound a, j), a: using MVD, b: using ligplot

### Acknowledgments

This research has been supported by Institute of Science and High Technology and Environmental Sciences, Graduate University of Advanced Technology (Kerman-Iran) under grant number of 99/1303.

### References

- [1] J. Gao, Z. Tian, X. Yang, Chloroquine phosphate has shown apparent efficacy in treatment of COVID-19 associated pneumonia in clinical studies, *Biosci. Trends*, 14, 72-73 (2020). <https://doi.org/10.5582/bst.2020.01047>
- [2] M. K. Gupta, S. Vemula, R. Donde, G. Gouda, L. Behera, R. Vadde, In-silico approaches to detect inhibitors of the human severe acute respiratory syndrome coronavirus envelope protein ion channel, *Journal of Biomolecular Structure and Dynamics*, 1-11 (2020). <https://doi.org/10.1080/07391102.2020.1751300>
- [3] F. Pan, T. Ye, P. Sun, S. Gui, B. Liang, L. Li, D. Zheng, J. Wang, R. L. Hesketh, L. Yang, Time course of lung changes on chest CT during recovery from 2019 novel coronavirus (COVID-19) pneumonia. *Radiology* (2020). <https://doi.org/10.1148/radiol.2020200370>
- [4] R. S. Joshi, S.S. Jagdale, S.B. Bansode, S.S. Shankar, M. B. TellisV. K. Pandya, A. Chugh, A. P. Giri, M. J. Kulkarni, Discovery of potential multi-target-directed ligands by targeting host-specific SARS-CoV-2 structurally conserved main protease. *Journal of Biomolecular Structure and Dynamics*, 1-16 (2020). <https://doi.org/10.1080/07391102.2020.1760137>
- [5] R. Sabino-Silva, A. C. G. Jardim, W. L. Siqueira, Coronavirus COVID-19 impacts to dentistry and potential salivary diagnosis, *Clinical oral investigations*, 24, 1619-1621 (2020). <https://doi.org/10.1007/s00784-020-03248-x>
- [6] Y. Wu, Y. C. Lu, M. Jacobs, S. Pradhan, K. Kapse, L. Zhao, N. Niforatos-Andescavage, G. Vezina, A. J. du Plessis, C. Limperopoulos, Association of prenatal maternal psychological distress with fetal brain growth, metabolism, and cortical maturation. *JAMA network open* 3, e1919940-e1919940 (2020). <https://doi.org/10.1001/jamanetworkopen.2019.19940>
- [7] A. A. Elfiky, E. B. Azzam, Novel guanosine derivatives against MERS CoV polymerase: An in silico perspective. *Journal of Biomolecular Structure and Dynamics*, 1-9 (2020). <https://doi.org/10.1080/07391102.2020.1758789>
- [8] A. D. Elmezayen, A. Al-Obaidi, A. T. Sahin, K. Yelekçi, Drug repurposing for coronavirus (COVID-19): in silico screening of known drugs against coronavirus 3CL hydrolase and protease enzymes, *Journal of Biomolecular Structure and Dynamics*, 1-13 (2020). <https://doi.org/10.1080/07391102.2020.1758791>
- [9] D. Zhou, S. M. Dai, Q. Tong, COVID-19: a recommendation to examine the effect of hydroxychloroquine in preventing infection and progression, *Journal of Antimicrobial Chemotherapy* 75, 1667-1670 (2020) <https://doi.org/10.1093/jac/dkaa114>
- [10] T. Kobayashi, S. M. Jung, N. M. Linton, R. Kinoshita, K. Hayashi, T. Miyama, A. Anzai, Y., Yang, B. Yuan, B., A. R. Akhmetzhanov, Communicating the risk of death from novel coronavirus disease (COVID-19). Multidisciplinary Digital Publishing Institute (2020). <https://doi.org/10.3390/jcm9020580>
- [11] H. Shi, X. Han, N. Jiang, Y. Cao, O. Alwalid, J. Gu, Y. Fan, C. Zheng, Radiological findings from 81 patients with COVID-19 pneumonia in Wuhan, China: a descriptive study. *The Lancet infectious diseases* 20, 425-434 (2020) [https://doi.org/10.1016/S1473-3099\(20\)30086-4](https://doi.org/10.1016/S1473-3099(20)30086-4)
- [12] C. C. Lai, T. P. Shih, W. C. Ko, H. J. Tang, P. R. Hsueh, Severe acute respiratory syndrome coronavirus 2 (SARS-CoV-2) and coronavirus disease-2019 (COVID-19): The epidemic and the challenges. *International journal of antimicrobial agents* 55, 105924 (2020). <https://doi.org/10.1016/j.ijantimicag.2020.105924>
- [13] K. Dong, S. Hu, J. Gao, Discovering drugs to treat coronavirus disease 2019 (COVID-19). *Drug discoveries & therapeutics* 14, 58-60 (2020). <https://doi.org/10.5582/ddt.2020.01012>
- [14] T. Y. Ling, M. D. Kuo, C. L. Li, L. Y. Alice, Y. H. Huang, T. J. Wu, Y. C. Lin, S. H. Chen, J. Yu, Identification of pulmonary Oct-4+ stem/progenitor cells and demonstration of their susceptibility to SARS coronavirus (SARS-CoV) infection in vitro. *Proceedings of the National Academy of Sciences* 103, 9530-9535 (2006). <https://doi.org/10.1073/pnas.0510232103>
- [15] V. K. Rao, S. S. Reddy, K. R. Babu, K. H. Kumar, S. K. Ghosh, C. N. Raju, Synthesis and cytotoxicity evaluation of phosphorylated derivatives of ribavirin, *Journal of the Korean Chemical Society* 55, 952-959 (2011). <https://doi.org/10.5012/jkcs.2011.55.6.952>
- [16] L. Ferretti, C. Wymant, M. Kendall, L. Zhao, A. Nurtay, L. Abeler-Dörner, M. Parker, D. Bonsall, C. Fraser, Quantifying SARS-CoV-2 transmission suggests epidemic control with digital contact tracing. *Science* 368 (2020). <https://doi.org/10.1126/science.abb6936>
- [17] R. J. Khan, R. K. Jha, G. M. Amera, M. Jain, E. Singh, A. Pathak, R. P. Singh, J. Muthukumaran, A. K. Singh, Targeting SARS-CoV-2: A systematic drug repurposing approach to identify promising inhibitors against 3C-like proteinase and 2'-O-ribose methyltransferase. *Journal of Biomolecular Structure and Dynamics*, 1-14 (2020).

- <https://doi.org/10.1080/07391102.2020.1753577>
- [18] W. Zhang, Y. Zhao, F. Zhang, Q. Wang, T. Li, Z. Liu, J., Wang, Y. Qin, X. Zhang, X. Yan, The use of anti-inflammatory drugs in the treatment of people with severe coronavirus disease 2019 (COVID-19): The Perspectives of clinical immunologists from China. *Clinical Immunology* 214, 108393 (2020).
- <https://doi.org/10.1016/j.clim.2020.108393>
- [19] G. Lu, Y. Hu, Q. Wang, J. Qi, F. Gao, Y. Li, Y. Zhang, W. Zhang, Y. Yuan, J. Bao, Molecular basis of binding between novel human coronavirus MERS-CoV and its receptor CD26. *Nature* 500, 227-231 (2013).
- <https://doi.org/10.1038/nature12328>
- [20] C. I. Paules, H. D. Marston, A. S. Fauci, Coronavirus infections—more than just the common cold, *Jama* 323, 707-708 (2020).
- <https://doi.org/10.1001/jama.2020.0757>
- [21] Z. Song, Y. Xu, L. Bao, Zhang, P. Yu, Y. Qu, H. Zhu, W. Zhao, Y. Han, C. Qin, From SARS to MERS, thrusting coronaviruses into the spotlight. *viruses* 11, 59 (2019).
- <https://doi.org/10.3390/v11010059>
- [22] I. T. Yu, Y. Li, T. W. Wong, W. Tam, A. T. Chan, J. H. Lee, D. Y. Leung, T. Ho, Evidence of airborne transmission of the severe acute respiratory syndrome virus. *New England Journal of Medicine* 350, 1731-1739 (2004).
- <https://doi.org/10.1056/NEJMoa032867>
- [23] P. A. Boley, M. A. Alhamo, G. Lossie, K. K. Yadav, M. Vasquez-Lee, M., L. J. Saif, S. P. Kenney, Porcine deltacoronavirus infection and transmission in poultry, United States. *Emerging infectious diseases* 26, 255 (2020).
- <https://doi.org/10.3201/eid2602.190346>
- [24] T. Li, Y. Cui, B. Wu, Molecular dynamics investigations of structural and functional changes in Bcl-2 induced by the novel antagonist BDA-366, *Journal of Biomolecular Structure and Dynamics* 37, 2527-2537 (2018).
- <https://doi.org/10.1080/07391102.2018.1491424>
- [25] D. A. Schwartz, A. L. Graham, Potential maternal and infant outcomes from (Wuhan) coronavirus 2019-nCoV infecting pregnant women: lessons from SARS, MERS, and other human coronavirus infections. *Viruses* 12, 194 (2020).
- <https://doi.org/10.3390/v12020194>
- [26] E. I. Azhar, D.S. Hui, Z. A. Memish, C. Drosten, A. Zumla, The middle east respiratory syndrome (MERS). *Infectious Disease Clinics* 33, 891-905 (2019).
- [https://doi.org/10.1016/S0140-6736\(15\)60454-8](https://doi.org/10.1016/S0140-6736(15)60454-8)
- [27] H. J. Berendsen, D. van der Spoel, R. van Drunen, GROMACS: a message-passing parallel molecular dynamics implementation. *Computer physics communications* 91, 43-56 (1995).
- [https://doi.org/10.1016/0010-4655\(95\)00042-E](https://doi.org/10.1016/0010-4655(95)00042-E)
- [28] M. Ebrahimi, T. Khayamian, Interactions of G-quadruplex DNA binding site with berberine derivatives and construct a structure-based QSAR using docking descriptors. *Medicinal Chemistry Research* 23, 1327-1339 (2014).
- <https://doi.org/10.1007/s00044-013-0733-y>
- [29] J. D. Durrant, J. A. McCammon, BINANA: a novel algorithm for ligand-binding characterization. *Journal of Molecular Graphics and Modelling* 29, 888-893 (2011).
- <https://doi.org/10.1016/j.jmgm.2011.01.004>
- [30] E. Estrada, G. Patlewicz, E. Uriarte, From molecular graphs to drugs. A review on the use of topological indices in drug design and discovery (2003).
- <http://hdl.handle.net/123456789/20663>
- [31] G. Bitencourt-Ferreira, W. F. de Azevedo, Molegro virtual docker for docking. *Docking Screens for Drug Discovery*. Springer, pp. 149-167 (2019).
- [https://doi.org/10.1007/978-1-4939-9752-7\\_10](https://doi.org/10.1007/978-1-4939-9752-7_10)
- [32] A. W. Schüttelkopf, D. M. Van Aalten, PRODRG: a tool for high-throughput crystallography of protein–ligand complexes. *Acta Crystallographica Section D: Biological Crystallography* 60, 1355-1363 (2004).
- <https://doi.org/10.1107/S0907444904011679>
- [33] D. M. Van Aalten, R. Bywater, J. B. Findlay, M. Hendlich, R. W. Hooft, G. Vriend, PRODRG, a program for generating molecular topologies and unique molecular descriptors from coordinates of small molecules. *Journal of computer-aided molecular design* 10, 255-262 (1996).
- <https://doi.org/10.1007/BF00355047>
- [34] S. Gharaghani, T. Khayamian, M. Ebrahimi, Multitarget fragment-based design of novel inhibitors for AChE and SSAO/VAP-1 enzymes. *Journal of Chemometrics* 27, 297-305 (2013).
- <https://doi.org/10.1002/cem.2556>
- [35] I. Halperin, B. Ma, H. Wolfson, R. Nussinov, Principles of docking: An overview of search algorithms and a guide to scoring functions. *Proteins: Structure, Function, and Bioinformatics* 47, 409-443 (2002).
- <https://doi.org/10.1002/prot.10115>
- [36] D. Hecht, M. Cheung, G. B. Fogel, Docking scores and QSAR using evolved neural networks for the pan-inhibition of wild-type and mutant PfDHFR by cycloguanil derivatives IEEE Congress on Evolutionary Computation. IEEE, 262-269 (2009).
- <https://doi.org/10.1109/CEC.2009.4982957>
- [37] J. D. Irvine, L. Takahashi, K. Lockhart, J. Cheong, J. W. Tolan, H. Selick, J. R. Grove, MDCK (Madin–Darby canine kidney) cells: a tool for membrane permeability screening. *Journal of pharmaceutical sciences* 88, 28-33 (1999).
- <https://doi.org/10.1021/js9803205>

## مطالعه داکینگ مولکولی چندین دارو با پتانسیل بر هم کنش با ویروس کرونا

داریوش افضلی<sup>۱\*</sup>، بهنوش بهادری<sup>۱</sup>، زهرا افضلی<sup>۲</sup>

۱- گروه محیط زیست، پژوهشکده علوم و فناوری عالی و علوم محیطی، دانشگاه تحصیلات تکمیلی فناوری پیشرفه، کرمان، ایران

۲- بخش نانوتکنولوژی، دانشگاه تحصیلات تکمیلی فناوری پیشرفته، کرمان، ایران

\* E-mail: daryoush\_afzali@yahoo.com

تاریخ دریافت: ۲۰ تیرماه ۱۴۰۳ | تاریخ پذیرش: ۱ شهریور ماه ۱۴۰۳

### چکیده

کرونا ویروس (COVID-19) جدید، SARS-COVID-2 در اوخر سال ۲۰۱۹ در ووهان، چین ظاهر شد و در سراسر جهان گسترش یافت. در این تحقیق، یک مطالعه بر روی COVID-19 و چندین مهار کننده بالینی انجام شده است، ابتدا شیوه سازی مولکولی COVID-19 Gromacs توسط ابزار انجام شد. سپس ترکیبات شیوه سازی شده با داروهای پیشنهادی برای تأیید داکینگ، داک شدند. نتایج داکینگ به مولکولی مشابه نتایج کریستالوگرافی اشعه ایکس در بانک داده پروتئین بود و تجزیه و تحلیل با این روش تأیید شد. ترکیب حاصل از داروهای گزارش شده با COVID-19 برای تجزیه و تحلیل متصل استفاده شد. علاوه بر این، برای مطالعه پایداری ترکیب گیرنده، یک شیوه سازی دوم بر روی مجموعه در یک محیط آبی انجام شد و RMSD به دست آمده برای کمپلکس، نشان داد که ترکیب COVID-19 در حضور داروهای پیشنهادی تغییری نداشته است. نتایج نشان داد که انرژی آزاد اتصال، انرژی بین مولکولی و پیوند هیدروژنی نقش مهمی در تعامل بین داروهای پیشنهادی و COVID-19-2 ایفا می کند. نتایج نشان داد که سوفوسیویر، ویتامین D و aurintricarboxylic 2- اسید به عنوان داروهای ضد ویروس کرونا COVID-19 بیشترین تأثیر را دارند.

کلید واژه ها: داکینگ مولکولی، دینامیک مولکولی، شیوه سازی

### COPYRIGHTS



© 2022 by the authors. Lisensee PNU, Tehran, Iran. This article is an open access article distributed under the terms and conditions of the Creative Commons Attribution 4.0 International (CC BY4.0) (<http://creativecommons.org/licenses/by/4.0>)